Control of the geometric phase with time-dependent fields

Xiaosong Zhu[1,2], Peixiang Lu[2] and Manfred Lein[1*]
[1] *Institut für Theoretische Physik, Leibniz Universität Hannover, D-30167 Hannover, Germany*
[2] *Wuhan National Laboratory for Optoelectronics and School of Physics, Huazhong University of Science and Technology, Wuhan 430074, China*
(Dated: October 16, 2019)

We evaluate the geometric phase acquired during the cyclic evolution of quantum systems exposed to time-periodic external fields, using Floquet theory and comparing the phase definition by Aharonov and Anandan to that by Berry. Ions in a light field and spin-1/2 particles in a magnetic field are considered. At high frequency, the Aharonov-Anandan phase converges to zero. In the limit of low frequency, it does not always converge to the adiabatic Berry phase, even though time evolution becomes adiabatic. Using a photon-channel perspective, we explain the oscillatory frequency dependence which facilitates control of the geometric phase. Control is also possible by steering the system through a degeneracy of the adiabatic energies, which can cause an additional phase of π. We demonstrate a robust example where both phase definitions agree and not only the dynamical phase but also the nonadiabatic corrections vanish at suitable frequencies.

When a quantum-mechanical system undergoes a closed circuit in parameter space, an adiabatically evolving state may acquire a geometric phase, known as the Berry phase [1], in addition to its dynamical phase, where the latter is essentially the time-integrated energy. Adiabaticity is usually satisfied under sufficiently slow parameter variation. It means that the quantum state remains close to an instantaneous eigenstate of the Hamiltonian at all times. The geometric phase has not only permeated through all branches of physics as an essential fundamental concept, but it has also inspired numerous cutting-edge applications [2–13]. Following Berry, the geometric phase can be evaluated from the instantaneous eigenstates by integration of the Berry connection, without reference to time evolution. However, since the adiabatic approximation is not necessarily valid for a cyclic process [14, 15], one may resort to the nonadiabatic generalization of the geometric phase by Aharonov and Anandan (AA) [16]. A conceptually different approach is the exact factorization of nonadiabatic molecular wavefunctions into nuclear and electronic functions [4, 17]. Focusing on the case of a Hamiltonian with time-varying parameter, we note that both Berry and AA consider the total phase acquired in a period T and subtract the dynamical phase θ, but they define the latter differently. Berry uses the time average $\bar{\mathcal{E}}_{\rm ad}$ of an instantaneous eigenenergy to define $\theta = -\bar{\mathcal{E}}_{\rm ad}T$ (written in atomic units); AA use the averaged energy expectation value $\bar{\mathcal{E}}$ to define $\theta = -\bar{\mathcal{E}}T$. Although in many applications, the two definitions agree in the adiabatic limit, one result of this Letter is the demonstration of a counter-example, calling for a discussion of the physical meaning.

A systematic way [18–20] to obtain the AA phase [21] follows from Floquet theory [22–24], the tool to describe periodically driven quantum matter [25, 26]. As temporal analog of the Bloch theorem, the Floquet theorem states that the time-dependent Schrödinger equation (TDSE) with a time-periodic Hamiltonian has cyclic-state solutions that return *exactly* to the initial state, up to an overall phase determined by the Floquet quasienergy. To investigate the adiabatic limit, it seems natural to consider Floquet states at low-frequency: the quasienergy can be written as a power series in frequency, where the linear term is zero except when there is a nonzero adiabatic Berry phase [27–33]. However, the low-frequency regime is highly nontrivial owing to multiphoton resonances, as we demonstrate below.

In this Letter, we scrutinize the frequency dependence of the geometric phase by considering four examples, involving a periodic laser field or magnetic field. A broad range of situations is covered: multiphoton resonances may be present, depending on the allowed quantum-mechanical transitions; the parameter circuit may lead through a degeneracy; the low-frequency Floquet states may or may not resemble adiabatically evolving states.

The time-dependent electric-field vector of a laser pulse follows a closed curve in the plane of polarization, i.e., it provides a closed loop in parameter space. The simplest example is a circularly polarized (CP) single-color field. The shape of the field can be controlled by using more than one color. In particular, bicircular fields, i.e., two-color fields with circularly polarized colors have recently been used for fundamental studies and novel applications [34–43], including the generation of CP extreme ultraviolet radiation [35] or the study of nonadiabaticity in strong-field ionization [43]. By admixture of a weak counter-rotating second color to the CP field, additional transitions become already possible and cause the appearance of multiphoton resonances, which we will interpret within a photon channel (PC) perspective [35, 44]. For a bicircular field with equal strengths of both colors, the field crosses zero several times per optical cycle. Such a 1:1 field can steer a system through a degeneracy if, as in many atomic ions, there are degenerate states at zero field strength. Although this does not hinder adia-

batic evolution, we find a breakdown of the equivalence between AA phase and Berry phase. Another relevant example, proposed already by AA [16] in the context of their nonadiabatic geometric phase, is a spin-1/2 particle in a time-dependent magnetic field that passes through zero once per cycle. Again, we find that the degeneracy does not prevent adiabatic evolution, but one must superpose different low-frequency Floquet states to retrieve the adiabatic state and to find equivalence between AA and Berry phases.

Floquet theory and geometric phase.—According to the Floquet theorem, the TDSE $\mathrm{i}\partial/\partial t|\Psi(t)\rangle = H(t)|\Psi(t)\rangle$ with periodic Hamiltonian $H(t) = H(t+T)$ has solutions $|\Psi(t)\rangle = e^{-i\mathcal{E}_f t}|P(t)\rangle$ with quasienergy $\mathcal{E}_f$ (dressed-state energy) and time-periodic states $|P(t+T)\rangle = |P(t)\rangle$ satisfying the Floquet equation $(H - i\partial/\partial t)|P(t)\rangle = \mathcal{E}_f|P(t)\rangle$. The total phase accumulation in one period is $-\mathcal{E}_f T$. Substracting the dynamical phase $-\bar{\mathcal{E}}T$ based on the time-averaged energy expectation value $\bar{\mathcal{E}} = \int_0^T \langle\Psi(t)|H(t)|\Psi(t)\rangle dt/T$, we obtain the AA phase $\gamma_A = (\bar{\mathcal{E}} - \mathcal{E}_f)T$. For practical calculations, the periodic state $|P(t)\rangle$ is expanded as a Fourier series $|P(t)\rangle = \sum_n e^{-in\omega t}|F_n\rangle$, $\omega = 2\pi/T$, so that the Floquet states are determined by a time-independent matrix eigenvalue equation [22, 23]. The AA phase takes the form $\gamma_A = 2\pi\bar{n}$ with $\bar{n} = \sum_n \langle F_n|F_n\rangle n$, see also [19, 29]. We interpret this result from the PC perspective: When an eigenstate of the field-free Hamiltonian is exposed to the external field, the initial state is a Floquet state with only $n=0$ populated. If the system remains in a single Floquet state while turning on the field, populations are redistributed by photon absorption/emission and $\langle F_n|F_n\rangle$ is the weight of the contribution reached by absorption of the photon energy $n\omega$. The AA phase equals the mean absorbed photon energy, in units of ω, multiplied by 2π. An alternative view on geometric phases is provided by low-frequency Floquet theory, where the quasienergy is expanded as $\mathcal{E}_f = \bar{\mathcal{E}}_{\mathrm{ad}} + \omega\mathcal{E}_f^{(1)} + \omega^2\mathcal{E}_f^{(2)} + \ldots$ [27–33] with $\bar{\mathcal{E}}_{\mathrm{ad}} = \int_0^T \mathcal{E}_{\mathrm{ad}}(t)dt/T$ and $\mathcal{E}_{\mathrm{ad}}(t)$ being an eigenvalue of $H(t)$. Using the dynamical phase $-\bar{\mathcal{E}}_{\mathrm{ad}}T$ as in [1], we find a Berry phase $\gamma_B = (\bar{\mathcal{E}}_{\mathrm{ad}} - \mathcal{E}_f)T$ including nonadiabaticity via $\mathcal{E}_f(\omega)$. The adiabatic Berry phase is given by the low-frequency limit $\gamma_B^{(0)} = -2\pi\mathcal{E}_f^{(1)}$. It can be observed by measuring the quasienergy. For example, positions of peaks in electron spectra from light-induced ionization depend on the bound-state quasienergies [45, 46].

Ne^+ ion in a light field.—This set of examples is motivated by the experimental feasibility of preparing ring-current states in rare-gas ions [47, 48]. We treat a single active electron in an effective potential [49] and we restrict the analysis to the $2p_\pm$ states with magnetic quantum numbers $m = \pm 1$ and the $2s$ state [50–52]. The bicircular electric field composed of frequencies ω and 2ω

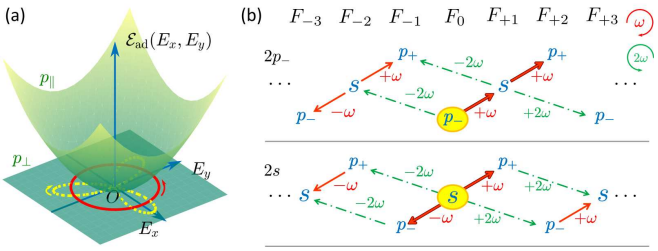

FIG. 1. (a) Energy surfaces of the electron $2p$ states in an electric field and paths of the electric field in the parameter space for the CP (red) and 1:1 bicircular (yellow) fields. (b) Illustration of the possible transitions in the bicircular field.

is

$$\mathbf{E}(t) = E_1[\cos(\omega t)\hat{\mathbf{e}}_x + \sin(\omega t)\hat{\mathbf{e}}_y] + E_2[\cos(2\omega t)\hat{\mathbf{e}}_x - \sin(2\omega t)\hat{\mathbf{e}}_y]. \quad (1)$$

A single-color CP field is a special case with $E_2 = 0$. The time-dependent Hamiltonian reads $H(t) = H_0 + \mathbf{r}\cdot\mathbf{E}(t)$. In one optical cycle, the field $\mathbf{E}(t)$ follows a closed circuit in a 2D parameter space (E_x-E_y-plane), see Fig. 1(a), which shows also the adiabatic eigenenergies $\mathcal{E}_{\mathrm{ad}}$ for the two $2p$ states as a function of the field. One of the orbitals tends to spatially align along the field (labeled $p_\parallel$), exhibiting a parabolic energy surface, whereas the other one tends to align perpendicularly (labeled $p_\perp$) with flat energy surface [50]. The degeneracy at $\mathbf{E} = 0$ is reminiscent of a Renner-Teller level touching, which shows no Berry phase when encircled by an adiabatic path [53]. In the Floquet calculation, we expand $|F_n\rangle = \sum_j c_{nj}|\phi_j\rangle$ where $|\phi_j\rangle$ are the field-free states ($j = p_-, s, p_+$). All solutions within an infinite set of quasienergies $\mathcal{E}_f' = \mathcal{E}_f + k\omega$ with integer k correspond to the same time-dependent state $|\Psi(t)\rangle$. Therefore, one obtains only three different states $|\Psi(t)\rangle$, describing the laser-dressed $2p$ and $2s$ states. Field-induced transitions are possible only within angular-momentum conservation rules. The possible PC from $2p_-$ and $2s$ as initial states are illustrated in Fig. 1(b). For a CP field, there are only few channels, indicated by the thick arrows.

The numerically calculated AA phases for a CP field with intensity $I = 5\times10^{14}$ W/cm^2 and variable ω are presented in Fig. 2(a) as a function of the dimensionless parameter $\mathcal{N} = 2D^2E_0^2/(\omega\Delta\mathcal{E})$, where $E_0^2 = E_1^2 + E_2^2$, $\Delta\mathcal{E} = 0.8509$ a.u. is the gap between the field-free $2p$ and $2s$ energies, and $D = \langle\phi_{p_\pm}|x|\phi_s\rangle = -0.3513$ a.u. We find nonzero γ_A with opposite signs for the $2p$ states, varying continuously from 0 at small $\mathcal{N}$ to $\pm2\pi$ at $\mathcal{N}\to\infty$, when we select the Floquet solutions with quasienergies close to $\bar{\mathcal{E}}$ at the smallest considered $\mathcal{N}$ [54]. It is intuitive that γ_A vanishes at large frequencies as there is no time ($T\to0$) to accumulate phase. To understand the low-frequency limit, we compare the Floquet state $|\Psi(t)\rangle$ with

the instantaneous eigenstates,

$$\Psi^{\rm ad}_{p_\parallel}(t) \propto (e^{2i\omega t}, \frac{e^{iwt}(\sqrt{\Delta\mathcal{E}^2+8D^2E_0^2}-\Delta\mathcal{E})}{2DE_0}, 1)^T \quad (2)$$

and $\Psi^{\rm ad}_{p_\perp}(t) \propto (-e^{2i\omega t}, 0, 1)^T$, where the three components are the expansion coefficients in the field-free states p_-, s, p_+, respectively. To this end, we evaluate the time-dependent fidelity $\mathcal{F}_j(t) = |\langle\Psi^{\rm ad}_j|\Psi(t)\rangle|^2$ and we define the adiabaticity indicator $\mathcal{F} = \max_j \min_t \mathcal{F}_j(t)$, plotted in Fig. 2(c). $\mathcal{F}$ converges to 1 for $\mathcal{N}\to\infty$ indicating low-frequency adiabatic behavior. Furthermore, since $|\langle\phi_{p_-}|\Psi^{\rm ad}_{p_\parallel}\rangle|^2 = |\langle\phi_{p_+}|\Psi^{\rm ad}_{p_\parallel}\rangle|^2 = (1-|\langle\phi_s|\Psi^{\rm ad}_{p_\parallel}\rangle|^2)/2$, the mean number of absorbed quanta ω when transiting from p_- (in Floquet channel $n=0$) to s and p_+ (cf. Fig. 1(b)) is $\bar{n}=1$, and $\gamma_A = 2\pi$ at $\omega\to 0$. In analogy, one finds -2π for the other p-type state. At intermediate $\mathcal{N}$, the system deviates from adiabaticity, resulting in nontrivial values of γ_A. For the $2s$ state, the PC from s to $p_\pm$ via absorbing/emitting photons are symmetric, so that $\bar{n}=0$ and $\gamma_A = 0$. Apparently, symmetry breaking of the PC for initial states carrying ring current causes nonzero geometric phases in this system. A similar conclusion drawn for pseudorotating molecules was that the nuclear ring currents allowed by a degeneracy play a crucial role in the nonzero geometric phase [17]. The adiabatic limit of the AA phase is (up to multiples of 2π) the same as the adiabatic Berry phase, obtained from the instantaneous eigenstates by integration of the Berry connection.

The geometric phase is reflected in the low-frequency behavior of the quasienergies. As shown in Fig. 2(e), the quasienergies of dressed p states converge to the adiabatic energies. In the special case of CP, we have $\bar{\mathcal{E}}_{\rm ad} = \mathcal{E}_{\rm ad}$. We find that the difference $\mathcal{E}_{\rm ad} - \mathcal{E}_f$ at $\omega\to 0$ is simply an integer multiple of ω, so that $\gamma_B^{(0)}$ is an integer multiple of 2π. Shifting $\mathcal{E}_f$ by a suitable amount $k\omega$ removes this trivial linear term and the shifted quasienergy $\tilde{\mathcal{E}}_f$, (yellow curve in Fig. 2(e)), converges to $\mathcal{E}_{\rm ad}$ (green line) quadratically in ω. In this case, the Berry phase $(\mathcal{E}_{\rm ad}-\tilde{\mathcal{E}}_f)T$ vanishes at $\omega\to 0$. Similarly, $\bar{\mathcal{E}}$ approaches $\tilde{\mathcal{E}}_f$ quadratically in ω, implying that γ_A approaches zero.

For a bicircular field with field-strength ratio 5:1 of the ω and 2ω components and total intensity $I = 5\times 10^{14}$ W/cm^2, nontrivial AA phases are again obtained for the ring-current $2p_\pm$ while $\gamma_A = 0$ for the $2s$ state, see Fig. 2(b). The most important new phenomenon is the appearance of multiphoton resonances. They cause avoided crossings of the quasienergy curves in Fig. 2(f). At a resonance, γ_A jumps by a large amount. The PC perspective explains this behavior. For example, at the avoided crossing between $|p_-,0\rangle$ and $|p_+,-1\rangle$, indicated by the first double-headed arrow in Fig. 2(f), the Floquet state emits the photon energy ω as n changes from 0 to -1. Additionally, as in the CP case, the difference between dressed state and field-free p_+ state implies slightly increased photon-energy emission so that γ_A drops below

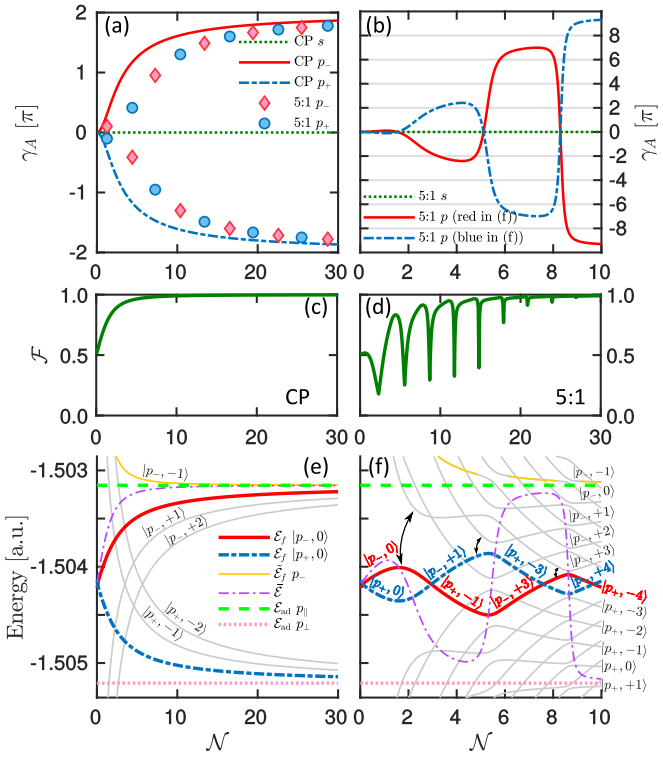

FIG. 2. (a),(b) AA phases for the CP and 5:1 bicircular fields. (Points have been shifted by integer multiples of 2π.) (c),(d) Adiabaticity indicator for p-type states. (e) Energy curves for the CP field. The label $|p_-,0\rangle$ denotes a solution for $|P(t)\rangle$ that resembles the p_- state at the smallest considered $\mathcal{N}$, while $|p_-,n\rangle$ denotes a solution with quasienergy differing by $-n\omega$. (f) Energy curves for the 5:1 bicircular field. The labels $|p_\pm,n\rangle$ refer to "diabatic" curves that would show as continuous lines in the absence of avoided crossings. In (e),(f), the dot-dashed curves correspond to the same Floquet states as the red curves.

-2π. Similarly, the state changes to $|p_-,+3\rangle$ at the second avoided crossing and γ_A jumps to above $3\times 2\pi$.

The adiabaticity indicator for the 5:1 bicircular field in Fig. 2(d) shows that the system is far from adiabaticity at resonances. At frequencies off resonances, we observe $\mathcal{F}\approx 1$ at large $\mathcal{N}$, as the p-type Floquet states approach either $\Psi^{\rm ad}_{p_\parallel}$ or $\Psi^{\rm ad}_{p_\perp}$ (calculated for the 5:1 field). In this sense, the system behaves adiabatically at low frequencies. We choose representative points in the middle between each pair of adjacent avoided crossings and plot the corresponding γ_A shifted by an integer multiple of 2π into the interval $[-2\pi,0]$ or $[0,2\pi]$, see Fig. 2(a), revealing a gradual change from 0 to $\pm 2\pi$, as in the CP field. At these points, also $|\bar{\mathcal{E}}-\tilde{\mathcal{E}}_f|$ and $|\bar{\mathcal{E}}_{\rm ad}-\tilde{\mathcal{E}}_f|$ decrease as ω^2 when $\omega\to 0$. Again, the phase obtained by integration of the Berry connection is an integer multiple of 2π. In short, $\gamma_A = \gamma_B$ in the adiabatic limit.

For the 1:1 bicircular field, the electric field (yellow curve in Fig. 1(a)) passes through zero three times per cycle. We find avoided crossings, see Fig. 3(a), and non-

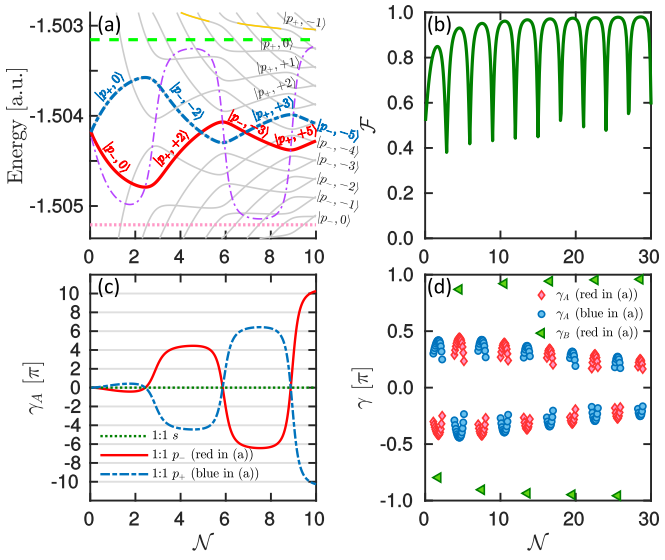

FIG. 3. (a-c) Same as Fig. 2(f,d,b) for the 1:1 bicircular field. (d) AA phase γ_A and Berry phase γ_B of $2p_-$ shifted by multiples of 2π.

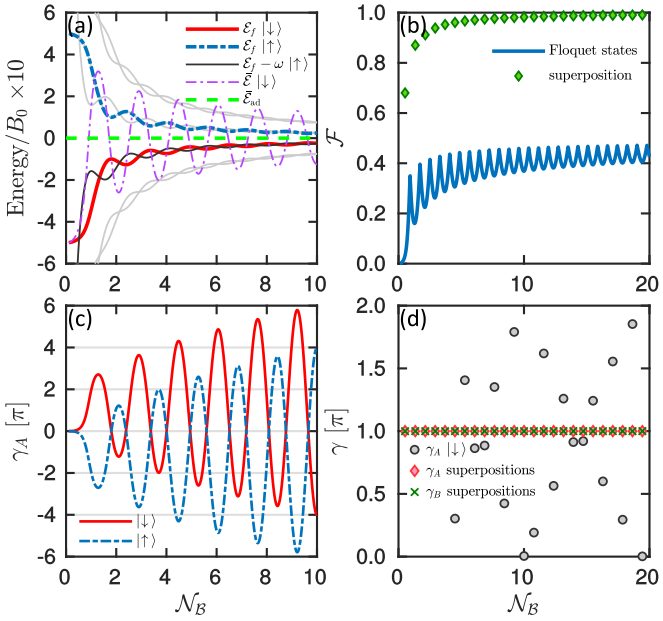

FIG. 4. (a) Energy curves for the spin-1/2 particle in a magnetic field. (b) Adiabaticity indicator for the Floquet states and superpositions. (c) AA phase for Floquet states. (d) AA phase γ_A and Berry phase γ_B shifted by multiples of 2π for a Floquet state and superpositions.

trivial AA phases of the p-type Floquet states, exhibiting phase jumps at the resonances, see Fig. 3(c). Figure 3(b) shows that the low-frequency evolution becomes adiabatic except at the avoided crossings. However, we find an anomalous behavior of γ_A, see Fig. 3(d), where a series of points between each pair of adjacent avoided crossings is selected and γ_A is shifted into $[-\pi,\pi]$. The AA phase does not seem to converge even when extending this calculation to $\mathcal{N}=900$, although $\bar{\mathcal{E}}$–$\tilde{\mathcal{E}}_f \to 0$ at $\omega \to 0$. For deeper understanding, we consider the instantaneous eigenstate $\Psi^{\rm ad}_{p_\perp}(t) \propto (-e^{-i\omega t},0,1)^T$. Unlike the examples without degeneracy, integration of the Berry connection yields $\pi \pmod{2\pi}$. Indeed, $\gamma_B = (\bar{\mathcal{E}}_{\rm ad}-\mathcal{E}_f)T$ calculated at points in the middle between avoided crossings also converges to $\pm\pi$, see Fig. 3(d). The striking conclusion is that AA phase and Berry phase differ in the adiabatic limit. At first sight, this may contradict the agreement of the two energies $\bar{\mathcal{E}}$ and $\bar{\mathcal{E}}_{\rm ad}$ at $\omega \to 0$. But in the dynamical-phase expressions $-\bar{\mathcal{E}}T$ and $-\bar{\mathcal{E}}_{\rm ad}T$, energies are multiplied with a diverging factor $T\to\infty$ and $|\bar{\mathcal{E}}-\tilde{\mathcal{E}}_f|$ does not decrease fast enough to let γ_A converge. The Berry phase π can be understood as follows. When the field goes through zero, its direction is suddenly reversed, whereas the aligned time-dependent wavefunction evolves continuously. After one cycle with N zero crossings, the field returns to its initial direction, whereas, relative to the field, the p-type wavefunction has reversed N times and therefore gained the phase $N\pi$. Hence, one can effectively control the geometric phase by steering the system though the degeneracy. Indeed, a 1:1 bicircular field with frequencies ω and $(N-1)\omega$ has N zero crossings [39] and $\gamma_B^{(0)} = N\pi \pmod{2\pi}$.

Spin-1/2 particle in a magnetic field.—We consider the time-varying field

$$\mathbf{B}(t) = B_0\hat{\mathbf{e}}_z + B_0[\cos(\omega_B t)\hat{\mathbf{e}}_z + \sin(\omega_B t)\hat{\mathbf{e}}_x], \quad (3)$$

describing a circle through zero. The Hamiltonian is $H(t) = \mathbf{B}\cdot\boldsymbol{\sigma}/2$ with the Pauli vector $\boldsymbol{\sigma}$. An aligned spin following the field direction cannot reverse suddenly when the field crosses zero. Thus, the system is expected to return to the initial state only after two rotations of the magnetic field [16]. We therefore choose the Floquet frequency $\omega = \omega_B/2$. For both instantaneous eigenstates $\Psi_1^{\rm ad}(t) = (\cos\frac{\omega t}{2}, \sin\frac{\omega t}{2})^T$ and $\Psi_2^{\rm ad}(t) = (-\sin\frac{\omega t}{2}, \cos\frac{\omega t}{2})^T$, the Berry connection results in an adiabatic Berry phase of π. The Floquet results are presented as a function of $\mathcal{N}_B = B_0/\omega_B$ in Fig. 4. We find Floquet states with avoided crossings and $\mathcal{F}$ is below 0.5, i.e., Floquet and adiabatic states differ strongly. Nevertheless, we can superpose two different Floquet states with equal weight at those frequencies where two quasienergies are equal, see the intersecting black and red curves in Fig. 4(a). The superpositions have $\mathcal{F}\approx 1$ at low frequency, i.e., their time evolution is adiabatic, see Fig. 4(b). While the Floquet states have strongly varying γ_A, see Fig. 4(c),(d), we find $\gamma_A = \gamma_B = \pi$ for the superpositions, surprisingly without frequency dependence. Here, $\gamma_A = \gamma_B$ because $\bar{\mathcal{E}} = \bar{\mathcal{E}}_{\rm ad} = 0$, implying zero dynamical phase.

Conclusion.—Our evaluation of the geometric phase for cyclic states reveals both surprises and useful features. Although the phase defined by Aharonov and Anandan

usually agrees with the adiabatic Berry phase in the low-frequency limit, we have presented a counter-example where they differ, although the time evolution is evidently adiabatic. Another example teaches us that low-frequency Floquet theory does not necessarily yield the adiabatic states directly, but these may be constructed by suitable superpositions. As the Berry phase determines the low-frequency expansion of the quasienergies, it has a direct relation to observable quantities. In view of applications of geometric phases in quantum information [55], it is of interest that our study suggests convenient control of geometric phases by tuning the driving frequency and by steering the system through degeneracies.

This work was supported by the Deutsche Forschungsgemeinschaft, the National Natural Science Foundation of China under Grants Nos. 11774109, 11627809, and the Alexander von Humboldt Foundation.

* lein@itp.uni-hannover.de

[1] M. V. Berry, "Quantal phase factors accompanying adiabatic changes," Proc. R. Soc. A Math. Phys. Eng. Sci. **392**, 45 (1984).

[2] A. Tomita and R. Y. Chiao, "Observation of Berry's topological phase by use of an optical fiber," Phys. Rev. Lett. **57**, 937 (1986).

[3] H. von Busch, Vas Dev, H.-A. Eckel, S. Kasahara, J. Wang, W. Demtröder, P. Sebald, and W. Meyer, "Unambiguous proof for Berry's phase in the sodium trimer: Analysis of the transition $A^2E'' \leftarrow X^2E'$," Phys. Rev. Lett. **81**, 4584 (1998).

[4] S. K. Min, A. Abedi, K. S. Kim, and E. K. U. Gross, "Is the molecular Berry phase an artifact of the Born-Oppenheimer approximation?" Phys. Rev. Lett. **113**, 263004 (2014).

[5] F. Bouakline, "Unambiguous signature of the Berry phase in intense laser dissociation of diatomic molecules," J. Phys. Chem. Lett. **9**, 2271 (2018).

[6] H. Liu, Y. Li, Y. S. You, S. Ghimire, T. F. Heinz, and D. A. Reis, "High-harmonic generation from an atomically thin semiconductor," Nat. Phys. **13**, 262 (2017).

[7] A. Chacón, W. Zhu, S. P. Kelly, A. Dauphin, E. Pisanty, A. Picón, C. Ticknor, M. F. Ciappina, A. Saxena, and M. Lewenstein, "Observing topological phase transitions with high harmonic generation," (2018), arXiv:1807.01616.

[8] R. E. F. Silva, Á. Jiménez-Galán, B. Amorim, O. Smirnova, and M. Ivanov, "Topological strong-field physics on sub-laser-cycle timescale," Nat. Photonics (2019), 10.1038/s41566-019-0516-1.

[9] L. Fu, C. L. Kane, and E. J. Mele, "Topological insulators in three dimensions," Phys. Rev. Lett. **98**, 106803 (2007).

[10] Y.-J. Lin, R. L. Compton, K. Jiménez-García, J. V. Porto, and I. B. Spielman, "Synthetic magnetic fields for ultracold neutral atoms," Nature **462**, 628 (2009).

[11] G. Hu, X. Hong, K. Wang, J. Wu, H. X. Xu, W. Zhao, W. Liu, S. Zhang, F. Garcia-Vidal, B. Wang, P. Lu, and C. W. Qiu, "Coherent steering of nonlinear chiral valley photons with a synthetic Au-WS_2 metasurface," Nat. Photonics **13**, 467 (2019).

[12] J.-S. Xu, K. Sun, J. K. Pachos, Y.-J. Han, C.-F. Li, and G.-C. Guo, "Photonic implementation of Majorana-based Berry phases," Sci. Adv. **4**, eaat6533 (2018).

[13] D. Xiao, M.-C. Chang, and Q. Niu, "Berry phase effects on electronic properties," Rev. Mod. Phys. **82**, 1959 (2010).

[14] S. Appelt, G. Wäckerle, and M. Mehring, "Deviation from Berry's adiabatic geometric phase in a Xe 131 nuclear gyroscope," Phys. Rev. Lett. **72**, 3921 (1994).

[15] X.-B. Wang and M. Keiji, "Nonadiabatic conditional geometric phase shift with NMR," Phys. Rev. Lett. **87**, 097901 (2001).

[16] Y. Aharonov and J. Anandan, "Phase change during a cyclic quantum evolution," Phys. Rev. Lett. **58**, 1593 (1987).

[17] R. Requist, F. Tandetzky, and E. K. U. Gross, "Molecular geometric phase from the exact electron-nuclear factorization," Phys. Rev. A **93**, 042108 (2016).

[18] D. J. Moore and G. E. Stedman, "Non-adiabatic Berry phase for periodic Hamiltonians," J. Phys. A. Math. Gen. **23**, 2049 (1990).

[19] D. J. Moore, "The calculation of nonadiabatic Berry phases," Phys. Rep. **210**, 1 (1991).

[20] J. Liu, B. Hu, and B. Li, "Nonadiabatic geometric phase and Hannay angle: A squeezed state approach," Phys. Rev. Lett. **81**, 1749 (1998).

[21] Moore and Stedman [18, 19] use the term "non-adiabatic Berry phase" for the AA phase. We reserve the term "Berry phase" for values obtained with Berry's definition of the dynamical phase.

[22] J. H. Shirley, "Solution of the Schrödinger equation with a Hamiltonian periodic in time," Phys. Rev. **138**, B979 (1965).

[23] C. J. Joachain, N. J. Kylstra, and R. M. Potvliege, *Atoms in intense laser fields* (Cambridge university press, New York, 2012) pp. 141–158.

[24] L. Medišauskas, U. Saalmann, and J. M. Rost, "Floquet Hamiltonian approach for dynamics in short and intense laser pulses," J. Phys. B At. Mol. Opt. Phys. **52**, 015602 (2019).

[25] H. Hübener, M. A. Sentef, U. De Giovannini, A. F. Kemper, and A. Rubio, "Creating stable Floquet-Weyl semimetals by laser-driving of 3D Dirac materials," Nat. Commun. **8**, 13940 (2017).

[26] R. Moessner and S. L. Sondhi, "Equilibration and order in quantum Floquet matter," Nat. Phys. **13**, 424 (2017).

[27] M. Pont, R. Shakeshaft, and R. M. Potvliege, "Low-frequency theory of multiphoton ionization," Phys. Rev. A **42**, 6969 (1990).

[28] M. Pont, R. M. Potvliege, R. Shakeshaft, and Z.-j. Teng, "Low-frequency theory of multiphoton ionization. II. General formulation and further results for ionization of H(1s)," Phys. Rev. A **45**, 8235 (1992).

[29] A. Russomanno, S. Pugnetti, V. Brosco, and R. Fazio, "Floquet theory of Cooper pair pumping," Phys. Rev. B **83**, 214508 (2011).

[30] H. Martiskainen and N. Moiseyev, "Perturbation theory for quasienergy floquet solutions in the low-frequency regime of the oscillating electric field," Phys. Rev. A **91**, 023416 (2015).

[31] H. Martiskainen and N. Moiseyev, "Adiabatic perturbation theory for atoms and molecules in the low-frequency

regime," J. Chem. Phys. **147**, 224101 (2017).
[32] A. Russomanno and G. E. Santoro, "Floquet resonances close to the adiabatic limit and the effect of dissipation," J. Stat. Mech. Theory Exp. **2017**, 103104 (2017).
[33] M. Rodriguez-Vega, M. Lentz, and B. Seradjeh, "Floquet perturbation theory: Formalism and application to low-frequency limit," New J. Phys. **20**, 093022 (2018).
[34] D. B. Milošević, W. Becker, and R. Kopold, "Generation of circularly polarized high-order harmonics by two-color coplanar field mixing," Phys. Rev. A **61**, 063403 (2000).
[35] A. Fleischer, O. Kfir, T. Diskin, P. Sidorenko, and O. Cohen, "Spin angular momentum and tunable polarization in high-harmonic generation," Nat. Photonics **8**, 543 (2014).
[36] L. Medišauskas, J. Wragg, H. van der Hart, and M. Y. Ivanov, "Generating isolated elliptically polarized attosecond pulses using bichromatic counterrotating circularly polarized laser fields," Phys. Rev. Lett. **115**, 153001 (2015).
[37] D. M. Reich and L. B. Madsen, "Illuminating molecular symmetries with bicircular high-order-harmonic generation," Phys. Rev. Lett. **117**, 133902 (2016).
[38] D. Baykusheva, S. Brennecke, M. Lein, and H. J. Wörner, "Signatures of electronic structure in bicircular high-harmonic spectroscopy," Phys. Rev. Lett. **119**, 203201 (2017).
[39] A. D. Bandrauk, J. Guo, and K.-J. Yuan, "Circularly polarized attosecond pulse generation and applications to ultrafast magnetism," J. Opt. (United Kingdom) **19**, 124016 (2017).
[40] Á. Jiménez-Galán, N. Zhavoronkov, D. Ayuso, F. Morales, S. Patchkovskii, M. Schloz, E. Pisanty, O. Smirnova, and M. Ivanov, "Control of attosecond light polarization in two-color bicircular fields," Phys. Rev. A **97**, 23409 (2018).
[41] O. Neufeld, D. Podolsky, and O. Cohen, "Floquet group theory and its application to selection rules in harmonic generation," Nat. Commun. **10**, 405 (2019).
[42] N. Eicke and M. Lein, "Attoclock with counter-rotating bicircular laser fields," Phys. Rev. A **99**, 031402(R) (2019).
[43] S. Eckart, K. Fehre, N. Eicke, A. Hartung, J. Rist, D. Trabert, N. Strenger, A. Pier, L. P. H. Schmidt, T. Jahnke, M. S. Schöffler, M. Lein, M. Kunitski, and R. Dörner, "Direct experimental access to the nonadiabatic initial momentum offset upon tunnel ionization," Phys. Rev. Lett. **121**, 163202 (2018).
[44] L. Li, P. Lan, L. He, X. Zhu, J. Chen, and P. Lu, "Scaling law of high harmonic generation in the framework of photon channels," Phys. Rev. Lett. **120**, 223203 (2018).
[45] M. Lein, E. K. U. Gross, and V. Engel, "Discrete peaks in above-threshold double-ionization spectra," Phys. Rev. A **64**, 023406 (2001).
[46] Y. H. Wang, H. Steinberg, P. Jarillo-Herrero, and N. Gedik, "Observation of Floquet-Bloch states on the surface of a topological insulator," Science **342**, 453 (2013).
[47] S. Eckart, M. Kunitski, M. Richter, A. Hartung, J. Rist, F. Trinter, K. Fehre, N. Schlott, K. Henrichs, L. Ph. H. Schmidt, T. Jahnke, M. Schöffler, K. Liu, I. Barth, J. Kaushal, F. Morales, M. Ivanov, O. Smirnova, and R. Dörner, "Ultrafast preparation and detection of ring currents in single atoms," Nat. Phys. **14**, 701 (2018).
[48] T. Herath, L. Yan, S. K. Lee, and W. Li, "Strong-field ionization rate depends on the sign of the magnetic quantum number," Phys. Rev. Lett. **109**, 043004 (2012).
[49] X. M. Tong and C. D. Lin, "Empirical formula for static field ionization rates of atoms and molecules by lasers in the barrier-suppression regime," J. Phys. B At. Mol. Opt. Phys. **38**, 2593 (2005).
[50] I. Barth and M. Lein, "Numerical verification of the theory of nonadiabatic tunnel ionization in strong circularly polarized laser fields," J. Phys. B At. Mol. Opt. Phys. **47**, 204016 (2014).
[51] X. Zhang, L. Li, X. Zhu, K. Liu, X. Liu, D. Wang, P. Lan, I. Barth, and P. Lu, "Subpetahertz helicity-modulated high-order harmonic radiation," Phys. Rev. A **98**, 23418 (2018).
[52] K. Liu, H. Ni, K. Renziehausen, J. M. Rost, and I. Barth, "Deformation of atomic $p_\pm$ orbitals in strong elliptically polarized laser fields: Ionization time drifts and spatial photoelectron separation," Phys. Rev. Lett. **121**, 203201 (2018).
[53] J. W. Zwanziger and E. R. Grant, "Topological phase in molecular bound states: Application to the $E \otimes e$ system," J. Chem. Phys. **87**, 1954 (1987).
[54] Very small $\mathcal{N}$ are excluded from Figs. 2,3 because of avoided crossings between s and p states that we do not discuss in the present work.
[55] E. Sjöqvist, "Geometric phases in quantum information," Int. J. Quantum Chem. **115**, 1311 (2015).